Three-Dimensional Image Sensing, Visualization, and Processing Using Integral Imaging

ADRIAN STERN AND BAHRAM JAVIDI, FELLOW, IEEE

Invited Paper

Three dimensional (3-D) imaging and display have been subjects of much research due to their diverse benefits and applications. However, due to the necessity to capture, record, process, and display an enormous amount of optical data for producing high-quality 3-D images, the developed 3-D imaging techniques were forced to compromise their performances (e.g., gave up the continuous parallax, restricting to a fixed viewing point) or to use special devices and technology (such as coherent illuminations, special spectacles) which is inconvenient for most practical implementation. Today's rapid progress of digital capture and display technology opened the possibility to proceed toward noncompromising, easy-to-use 3-D imaging techniques. This technology progress prompted the revival of the integral imaging (II) technique based on a technique proposed almost one century ago. II is a type of multiview 3-D imaging system that uses an array of diffractive or refractive elements to capture the 3-D optical data. It has attracted great attention recently, since it produces autostereoscopic images without special illumination requirements. However, with a conventional II system it is not possible to produce 3-D images that have both high resolution, large depth-of-field, and large viewing angle. This paper provides an overview of the approaches and techniques developed during the last decade to overcome these limitations. By combining these techniques with upcoming technology it is to be expected that II-based 3-D imaging systems will reach practical applicability in various fields.

Keywords—Computer-generated integral imaging (CGII), computational integral imaging (CII), integral imaging (II), three-dimensional (3-D) imaging.

I. INTRODUCTION

Three dimensional (3-D) imaging and visualization techniques have been the subject of research for many years. It was in 1828 when Sir Wheatstone introduced a stereoscopic viewing device known as the "mirror stereoscope" [1]. Because photography was unknown at the time,

drawings were used. Since then, technology has advanced and numerous 3-D imaging techniques were developed, each having its advantages and disadvantages. Among 3-D imaging techniques, an integral imaging (II) system is a promising technology because: 1) it produces autostereoscopic images, thus not requiring special viewing devices; 2) it provides the observer images with full parallax and continuous viewing points; 3) it is passive; i.e., it does not require special illumination of the scene; 4) it can operate with regular incoherent daylight; 5) its system configuration is compact; 6) its implementation is relatively simple.

The most widely used 3-D imaging technique to date is still the stereoscopic technique based on Sir Wheatstone's "mirror stereoscope" concept. II is well contrasted with the stereoscopic techniques, which usually require supplementary glasses to evoke a 3-D visual effect to observers [2]. Moreover, in stereoscopic techniques, observers see only a fixed viewpoint and may experience visual fatigue because of convergence-accommodation conflict [3]. Holography does not suffer from these problems, as it generates 3-D images with full parallax and continuous viewing. However, holography involves coherent illumination, which makes the imaging system more complicated, expensive, and sensitive to various factors.

A. Principle of Operation

Before describing the principle of operation of an II system we shall describe first a model of an ideal 3-D imaging system [4]. Such a system is described heuristically in Fig. 1(a). If the entire information (directions, intensities, wavelength, state of polarization, etc.) of the rays originating from a 3-D object is recorded on a boundary surface surrounding the 3-D object [i.e., the cylinder S in Fig. 1(a)], a 3-D image of the object can be reconstructed for any viewing point by generating rays of the same direction and intensity. As shown in Fig. 1(a), the boundary surface divides a 3-D space into two spaces: one in which the viewer is located in (viewing space) and other is the space in which the object is located (visual space). Practically, the boundary
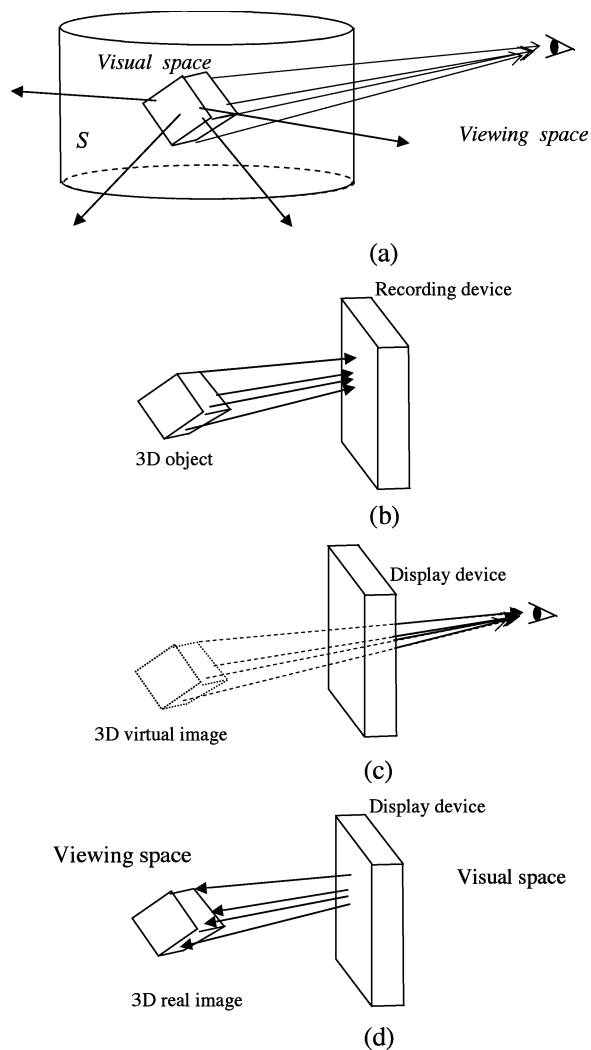
Fig. 1. (a) An ideal 3-D imaging. All the rays emerging form the 3-D object need to be captured on a boundary surface S. (b) Light rays from a 3-D object are collected by a planar recording device. (c) 3-D virtual image is formed by exactly continuing the rays. (d) 3-D real image is formed by continuing the rays in opposite direction forming a real image. Note that the visual and viewing spaces are horizontally flipped in this figure with respect to those in (a).

surface is in general not closed, as for example in Fig. 1(b). In Fig. 1(b) the rays are collected by a planar recording device on a finite area. This is the case of the conventional II systems. In the image reconstruction step, rays having exactly the same directions as those of the recording rays [Fig. 1(c)] are generated to form a virtual orthoscopic image. It is possible to generate rays that are exactly opposite to those of the recording rays. In such a case a pseudoscopic (depth-reversed) real image is obtained [Fig. 1(d)].

Conventional II systems typically sample the rays on a planar surface such as that in Fig. 1(b) by using an aperture (pinhole) plate or a lenslet (microlens) array. The sampled rays are recorded on photographic film or by digital means such as by a CCD or CMOS camera. For reconstruction, another aperture or lenslet array is used to continue the ray propagation [Fig. 1(c) and (d)]. The typical setup of an II system is described in detail in Section II.

Typically the pitch of the lenslet or aperture plate is relatively small (typically around 1 mm); therefore' II can be considered as a 3-D multiview imaging system with a dense sampling ray rate. However, the ray sampling rate is finite, which together with limitation of the optical components of an II system, set limitations on the performance of the system. Those limitations are described in Section III.

Hence one way to interpret II systems is as systems that sample and reconstruct the optical field emerging form the 3-D object. A useful tool for describing the behavior of the lenslet array as a ray field sampler together with describing the nongeometrical effects is the ray phase space (RPS), which is presented in [4]. The RPS is a four-parameter space-angle representation of the optical data captured at surface S. An alternative way to interpret II systems is as a spatial multiplexing scheme of conventional imaging systems [5]. II systems can be viewed as multichannel imaging systems, each channel arising from a conventional single aperture imaging system. The multitude of channels may provide several benefits [5]; the most important for 3-D imaging is the ability to capture multiview images.

B. History of Development

II was invented in 1908 by Nobel price laureate G. Lippmann [6] and was originally named integral photography (IP). The term "integral imaging" was introduced recently to reflect the imaging and image processing nature of modern applications [7]. The history of development of IP can be found in [2] and [8]. Here we will mention only a few milestones. First experiments were done by Sokolov in 1911 using a pinhole array [9]. Experiments with lenslet arrays could not be performed before World War II because good plastic materials were not available. In the late 1920s lenticular sheets were considered as simplification of IP. "Lenticule" is a synonym for "lens," but has come to mean a sheet of long thin lenses. Lenticular sheets contain a series of cylindrical lenses, today molded into a plastic substrate. Lenticular sheets are easier to manufacture, but when used instead of the lenslet array in IP systems, one needs to give up the vertical parallax. Ives [10] in 1931 pointed that an IP produces a pseudoscopic image, that is, an image inverted in depth. To solve this problem, he proposed a method called "two-step IP" with which a second IP of the reconstructed image obtained with Lippmann's method is produced. In such a scheme, although the image is deteriorated in resolution, it is no longer pseudoscopic but orthoscopic. Beside a few studies in the 1960s and 1970s [2], IP did not gain much interest because technology of image recording and display and of lenslet array manufacturing was not mature for practical IP realization. It was only in the last decade when technology has approached the level required for practical realization. The availability of high-resolution light-sensitive devices, such as high-resolution CCDs, replaced the photographic plate and enabled further applications that involve electronic transmission and reconstruction of 3-D images [11]–[15], computerized reconstruction and recognition [7], [16]–[22] of 3-D objects by means of digital

image processing, and efficient storage by digital compression [23], [24] of the recorded images. Since the rebirth in 1997 by Okano *et al.* [11], many important theoretical and experimental contributions have been reported, the main ones described in this paper.

C. Applications

There are numerous applications where the ability to capture, display, and visualize 3-D images comfortably would confer real benefits. Examples from the professional domain include computer-aided design, medical imaging, scientific visualization, and remote inspection; while in the consumer markets the likes of 3-D television, 3-D video games, and 3-D multimedia, interactive shopping, interior design, edutainment (education + entertainment), and advertisement have a clear mass market appeal. Recently numerous studies have been carried out and techniques were developed that promote II toward application in the professional and consumer field.

The trigger for the recent revival of II was introducing digital capture [11] and display devices in the traditional IP system. This offers the possibility of transmitting, shooting moving pictures, digital processing, and storage of the images captured. In the field of entertainment, although II has not yet reached the technology level required for commercial application, large steps are being taken toward it. It is likely that with coming generations of digital display and capturing devices, 3-D imaging and display techniques based on II principle will find their application in this field.

Several applications of II were proposed in various fields. The additional dimension captured by an II system may enhance the performance of traditional 2-D pattern recognition techniques. Several techniques to passively sense, detect, and recognize 3-D objects using II were developed [16], [21], [25]–[30]. Experiments demonstrate that 3-D recognition algorithms are more discriminant than two-dimensional (2-D) ones [16].

A technique to display 3-D micro-objects in space using II was presented in [31]. The technique was demonstrated for visualizing 3-D images of biological specimens having a size of approximately 18×40 μm, captured with confocal (laser scanning) microscopy [32]. Such a method can assist physicians, biologists, scientists, and engineers to perceive the 3-D structure of micro-objects more vividly and accurately.

A real-time animated version of II, called integral videography, was developed in [33] for surgery navigation. The surgeon sees an actual 3-D image superimposed onto the patient using a semitransparent display based on the II technique. He is guided by indicating the location of a tracking device through cross-sectional images, for X-ray computed tomography and/or magnetic resonance images. By localizing the targeted lesion and the critical lesion that should be avoided, surgical navigation using integral videography helps to achieve safe surgery while minimizing the invasiveness of the surgery. Errors in the range of 2–3 mm were found experimentally. The accuracy of the technique could be increased with the next generation of displays, or alternatively by using methods described in [31] and [34].

D. Scope of This Paper

In this paper we will provide an updated overview of recent advances in II technology. The paper is intended to help the reader to identify the bottlenecks in specific II systems and to familiarize him with approaches and existing techniques to overcome them.

In Section II we describe and classify common II systems. In Section III we analyze briefly the performance of II and define figures of merit that could help to optimize II systems and to compare between specific implementations. The tradeoff between resolution, viewing zone, and depth of field is identified. Then in Section IV we present a multiplexing approach to increase the total information of the system, which, if followed by techniques presented in Section V, can be used to improve the performance of II with respect to desired parameters.

II. CLASSIFICATION OF II SYSTEMS

Here we present a primary classification of II systems based on distinguishing between optical and digital image formation, capturing or synthesis. Other classifications based on type of components of the II system or based on type of application are equally possible.

A. Full Optical II

A typical II system is shown schematically in Fig. 2. In the II pickup (recording) process the direction and intensity information of the rays coming from a 3-D object is spatially sampled by use of a lenslet (or pinhole lens) array and recorded by a 2-D image sensor as depicted in Fig. 2(a). The ray information sampled by each lenslet (or pinhole lens) is a demagnified 2-D image with its own perspective, referred to as an elemental image, which is captured by a recording device such as a CCD or CMOS sensor.

In the reconstruction process, the recorded 2-D elemental images are displayed by a 2-D display panel, such as a liquid crystal display (LCD) panel, and the rays coming from the elemental images are redirected to form a real 3-D image as depicted in Fig. 2(b). In Fig. 2(b) we assume that the distance g_d between the recording device and the lenslet is larger than the lenslet focal length f_l; $g_d > f_l$. This 3-D image is a pseudoscopic (depth-reversed) image of the 3-D object. The pseudoscopic real image can be converted into an orthoscopic virtual image [Fig. 2(c)] by flipping every elemental image around its own center optic axis. Such pseudoscopic–orthoscopic conversion can be accomplished either optically [10], [12], [34], [35] or digitally [12], [34]. Some of the optical pseudoscopic–orthoscopic conversions [10], [12] involve some image degradation. Orthoscopic virtual images can be obtained directly also by setting $g_d < f_l$ [37]. It is also possible to display an orthoscopic real image by introducing an additional imaging lens in front of the pickup lenslet array [38].

B. Computational II (CII)

CII is often used, in which a 3-D image is generated in a computer using elemental images picked up by a CCD rather than optical reconstruction using an LCD and lenslet array [7],
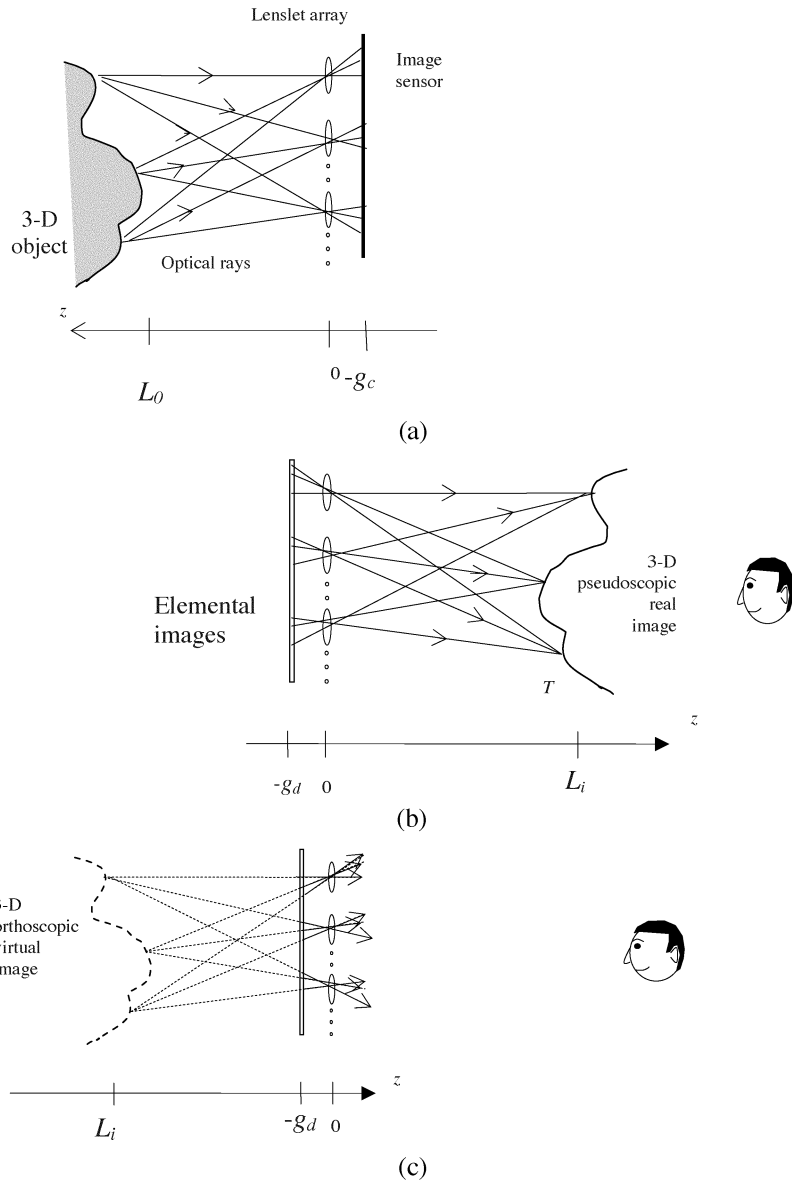
Fig. 2. Conventional II with planar devices. (a) Pickup. (b) Real image display. Lenslet focal length f_l is assumed to be smaller than the gap g_d. (c) Virtual image display.

[17]–[22]. Two approaches are used for CII image restoration. By one approach [7], [17], [19], [20] a hypothetical pinhole array is used to simulate the display process depicted in Fig. 2(c), according to a ray tracing approach. By the other, the disparity between elemental images is used to generate depth cross-sections of the 3-D image [16], [21], [22].

The quality of the synthesized image using CII reconstruction is better than that of the images reconstructed using all-optical II. This is because CII reconstruction is free of diffraction and device limitations, and of system misalignment, even if there are truncation errors due to the digitally computed inverse mapping. The reconstructed image is inherently reconstructed to be orthoscopic. The obvious disadvantage of CII over optical II is that it produces only one view at a time.

C. Computer-Generated II (CGII)

Similar to CII, the pickup process can be simulated by a computer, and computer-generated integral images can be displayed optically by an LCD [33], [39]–[43]. Thus, the process in Fig. 2(a) is performed by a computer using a ray tracing method and the reconstruction in Fig. 2(b) or (c) is carried out optically. The pseudoscopic–orthoscopic conversions are included in the digital process.

III. PERFORMANCE ANALYSIS OF II

There are a number of factors that impact the quality of 3-D reconstruction. These include diffraction due to the small size of the lenslets, limited sampling rate due to the finite pitch of the lenslet array, imperfections of optical sensor in the pickup process, limited sampling rate of the recording and display device, and truncation errors due to the limited dynamic range of digital devices involved. Numerous studies were carried out to determine the impact of these and other factors on II performance [11], [22], [44]–[55]. In the following we will summarize the main results. To simplify the mathematical expressions, we will limit our discussion to
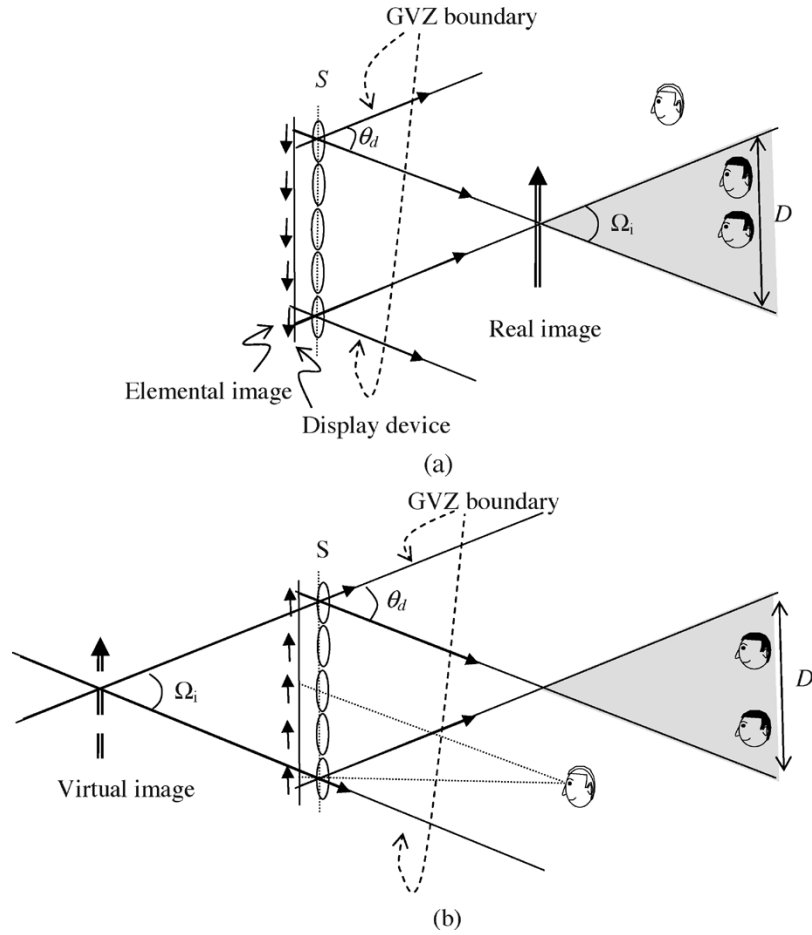
Fig. 3. Viewing zone (shaded area), viewing zone width D, general viewing zone, and maximal viewing angle VA$_i$ Ω_i for: (a) real integral image (bold arrow) and (b) virtual integral image (dashed arrow).

one-dimensional II. The extension of the presented analysis to 2-D II is straightforward.

A. Geometrical Viewing and Visual Specifications

The concept of viewing zone and viewing angle are of essential importance in autostereoscopic 3-D display [2]. The *viewing zone* (VZ) is defined as the movable range in the viewing space (Fig. 1) where the viewer can see a full resolution image; that is, he can see rays emitted from the entire surface area S (display lenslet array in the II case). The VZ has to be as wide as possible to enable as many viewers as possible to simultaneously view the 3-D scene. Typically the VZ is quantified by its lateral cross section width D at a given distance from the display. For a typical II system, as shown in Fig. 3, the VZ is determined by the display lenslet exit full angle given by

$$\theta_d = 2 \tan^{-1}\left(\frac{p_d}{2g_d}\right) \qquad (1)$$

where p_d is the display lenslet pitch and g_d is the gap between the display plane and the lenslet array (Fig. 2). This is the maximal angle of ray that can be generated by an elemental image and imaged from its assigned lenslet.

We define *general viewing zone* (GVZ) as the movable range where a viewer can see at least one image point. The GVZ for common II display is shown in Fig. 3. Viewers located in the GVZ but outside the VZ see distorted or flipped images because part of the rays seen are seen through lenslets adjacent to the lenslet corresponding to the elemental image point generating the ray. To prevent this, the elemental image that exceeds the corresponding area is discarded optically in the direct pick up method (see Section V-A) or electrically in the CGII method. In such a case viewers outside the VZ that are still in the GVZ, such as the bright hair viewers in Fig. 3(a) and (b), see a truncated image because they cannot see all the elemental images. As can be seen in Fig. 3, the GVZ is also dictated by the lenslet exit angle θ_d.

The *image viewing angle* (VA$_i$) is defined as the range of directions from which an image point can be seen. The image viewing angle depends on the image location, on the display lenslet array size and lenslet exit angle θ_d. For a given II display, the image viewing angle depends on the image locations; therefore, we will refer to the *maximum* image viewing angle Ω_i as a figure of merit of the display system. In Fig. 3 the image is placed in the location from which its central point can be seen from the largest range of directions. It can be seen that for the conventional II system in Fig. 3, the maximum VA$_i$ equals the lenslet exit angle $\Omega_i = \theta_d$. Thus, we
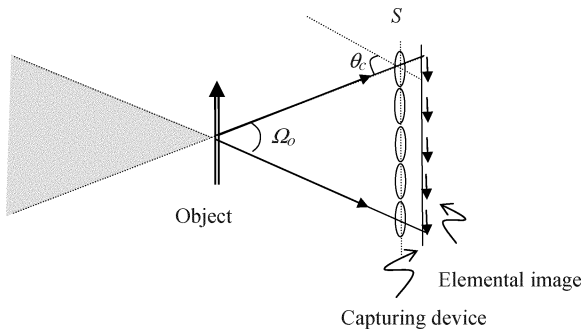
Fig. 4. Visual field (shaded area), and object maximal viewing angle Ω_o.

see that for the II system in Fig. 3, the VZ equals the maximum VA_i; therefore, often the VZ is defined through the maximum VA_i. In general, if the 3-D imaging system has a planar and uniform display surface S, the VZ and GVZ are closely related to the maximum VA_i.

Thus we see that the lenslet exit angle θ_d defines the viewing geometry. With a typical II display setup, g_d is approximately the lenslet focal length and the lenslet fill factor is close to one, so that the pitch p_d equals approximately the lenslet aperture. Therefore, in general, from (1), $\theta_d \approx 2NA = 1/F\#$, where NA and $F\#$ denote the numerical aperture and f-number of the lenslet, respectively. Thus, we can conclude that for common II the VZ, GVZ, and maximum VA_i are proportional to the display lenslet NA and inversely proportional to their $F\#$.

In addition to the image viewing geometry, the object capturing space geometry needs to be defined also: the geometry of captured rays in the visual space in Fig. 1. The need to define the capturing geometry is obvious if we consider a CII system for which the viewing geometry is virtual and therefore we are primarily concerned with the object location and angles that it can be captured from. We define the *object visual field* (VF$_o$) as the spatial region where object points are "seen" and captured from the entire capturing surface S. The term "visual" is often used (or meant) with respect to "seeing" geometry of an *image*; therefore, we emphasize here that we refer to *object* visual field. The VF$_o$ for a conventional II system is shown in Fig. 4. It depends on the capturing lenslet array size and capturing lenslet exit angle θ_c given by $\theta_c = \tan^{-1}(p_c/g_c)$, where p_c is the display lenslet pitch and g_c is the gap between the display plane and the lenslet array (Fig. 2). As with the display II subsystem, the capturing lenslet array exit angle is in general given by twice the capturing lenslet NA or by $1/F\#$: $\theta_c \approx 2NA = 1/F\#$.

We define the *object viewing angle* VA$_o$ as the angular range that an *object* point is "seen" by the capturing system, that is, the angle subtended by the capturing surface S relative to the object point. Typically VA$_o$ depends on the capturing lenslet exit angle θ_c and the location of the object. As a figure of merit of the capturing system, we use the *maximum* VA$_o$ obtained from an object point located at the position from which is "seen" by the capturing system in the widest range of directions. The maximum VA$_o\Omega_o$ for a conventional II capturing system is shown in Fig. 4. It can be

seen that $\Omega_o = \theta_c$. Thus, for an II system with planar and uniform lenslet array the VA$_o$ and the VF$_o$ are dictated by the capturing lenslet array NA or alternatively by their $F\#$. In some cases relay optics are located between the pickup lens array and the capturing sensor, which may reduce the maximum VA$_o$ due to vignetting [56].

If an II system has symmetrical capturing and displaying subsystems—that is, they have the same lenslet array specifications, same optical setup, same recording and display devices resolution and size—then the maximum VA$_i$ equals the maximum VA$_o$ and the VZ is a mirror of the VF$_o$. However, if the overall II system performs magnification, or nonplanar lenslets are used or if vignetting is induced by some relay optics, then the values of the terms characterizing the capture and display may differ.

B. Lateral Resolution

To evaluate the resolution of II systems, one can adopt an optical transfer function (OTF) analysis [44], [45], [54], [57]. Strictly speaking such an analysis is not valid, since OTF analysis holds only for linear shift invariant systems, which II is not. A principal reason for not being linear shift invariant is because of the sampling processes involved in the recording and display stages, which are space-variant. However, to preserve the convenience of the transfer function approach, it is possible to define a spatially averaged optical transfer function (AOTF) [55] by assuming that the sampled image is randomly positioned with respect to the sampling grid location. Thus, even though II is not a linear shift invariant system, a fair estimate of its resolution can be obtained through the elegant OTF analysis approach.

For CII the resolution is determined solely by the capturing system OTF, which is given by the product of the pickup lenslet array OTF and pickup device lenlslet array. For a full-optical II, the overall system OTF (capture and display) needs to be considered [46], [55], [57]. The OTF for a capture and display system using a square aperture or lens array is given in [45]. The OTF for systems using a circular aperture can be found in [46].

The maximum spatial angular resolution α_c [in cycles/rad (cpr)] that can provide a capture, a display, or capture-and-display system can be defined as the cutoff angular spatial frequency of the system modulation transfer function (MTF) [55] given by $\text{MTF}(\alpha) = |\text{OTF}(\alpha)|$. An example of an MTF of a capturing II system is shown in Fig. 5(a). The cutoff frequency of the overall MTF in Fig. 5(a) is $\alpha_c = 250$ cpr. The main limiting sources of α_c are diffraction due to finite lenslet aperture, focusing errors, and the sampling process when digital capturing and/or display devices are used. Accordingly the cutoff frequency of a capturing system α_c using a lenslet array can be approximated by [45], [46], [55], [57]

$$\alpha_c = \min(\alpha_{\text{cdiff}}, \alpha_{\text{cerrf}}, \alpha_{\text{cd}}) \tag{2}$$

where α_{cdiff} is the diffraction limit cutoff frequency, α_{cd} is the capturing device cutoff frequency, and α_{cerrf} is the cutoff
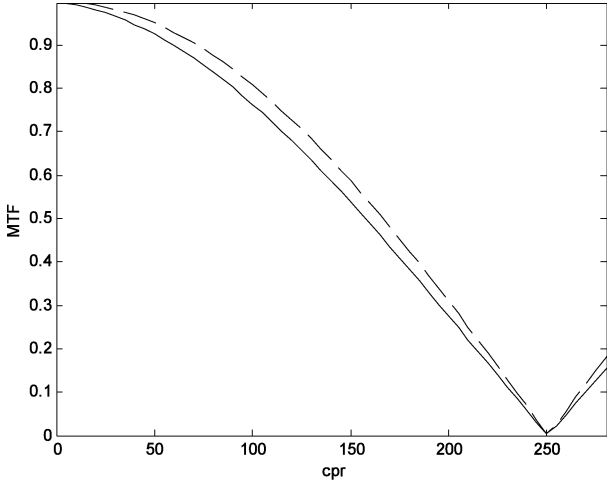
(a)
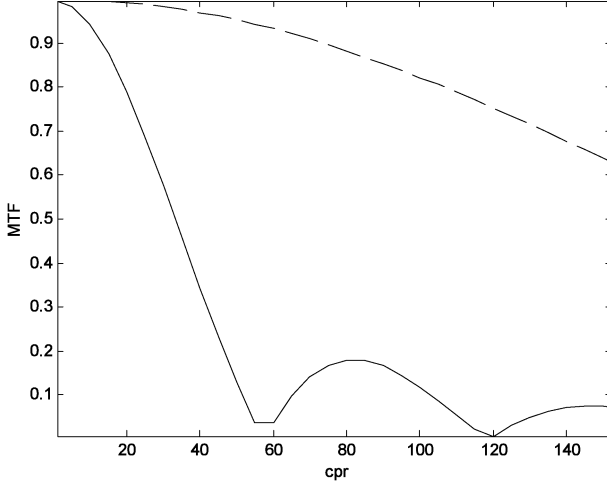
(b)

Fig. 5. Overall MTF (solid line) of typical II capturing system ($f_l = 5$ mm, $p_d \approx w_{cl} = 1$ mm, $p_{cpxl} = 10$ μm, $L_0 = 0.5$ m). (a) In-focus system. The overall MTF (solid line) is determined mainly by the sampling average MTF (dashed line). The diffraction MTF (doted line) is much higher then the sampling average MTF. (b) Overall MTF (solid line) of severely out-of-focus system. The system is focusing at 0.5 m whereas the object is at distance $L_0 = 0.05$ m in front of the lenslet array. The out-of-focus MTF (dotted line) is much lower then sampling MTF (dashed line).

frequency due to the defocusing. For square aperture lenslets α_{cdiff} is given by [45]

$$\alpha_{cdiff} = \frac{w_{cl}}{\lambda} \qquad (3)$$

where w_{cl} is the lenslet aperture and λ is the light wavelength. In general α_{cerrf} dominates only in very severely out-of-focus situations such as the one depicted in Fig. 5(b). In such cases [45]

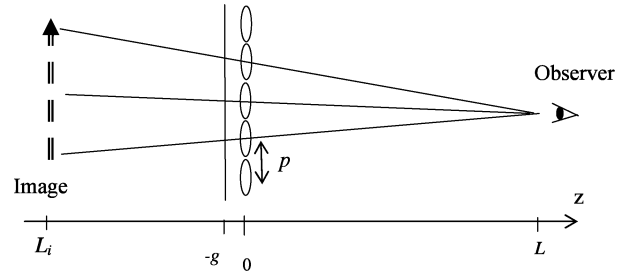$$\alpha_{cerrf} \approx \frac{1}{w_{cl} e_{cerr}(z)} \qquad (4)$$

Fig. 6. Sampling of the reconstructed image.

where $e_{cerr}(z)$ is the focusing phase which depends on the object plane z, lenslet focal length f_{cl}, and gap between the lenslet-array and the optics pickup focusing g_c

$$e_{ecrr}(z) = \left| \frac{1}{z} + \frac{1}{g_c} - \frac{1}{f_{cl}} \right|. \qquad (5)$$

If a pixilated capturing device is used and the lenslet aperture is large enough so that $\alpha_{cdiff} \gg \alpha_{cd}$ then the capturing device cutoff frequency is approximately [55]

$$\alpha_{cd} = \frac{g_c M}{2 p_{cpxl}} \qquad (6)$$

where p_{cpxl} is the pixel sensor size, M is lateral magnification of the pickup optics typically located between the lenslet array and the CCD, and g_c is the gap between the lenslet array and the pickup optics imaging plane. In the example of Fig. 5, $\alpha_{cdiff} = 1800$ cpr, $\alpha_{cd} = 250$ cpr, and, since the object is in focus, $\alpha_{cerrf} = \infty$. In the example of Fig. 5(b), the object is severely out of focus and $\alpha_{cerrf} = 60$ cpr.

With a CII system the resolution is limited only during the capturing process; therefore, it is determined by (2). However, with a full-optical II system, the resolution may be further degraded by the optical display system so that the overall system cutoff frequency α_T is

$$\alpha_T = \min(\alpha_c, \alpha_d) \qquad (7)$$

where α_d is the display cutoff frequency, which can be calculated in a similar way to (2)–(6) by substituting the appropriate display system dimensional parameters.

The cutoff spatial frequency α_T can be regarded as the angular frequency of the rays emitted from the lenslets during image reproduction. From Fig. 6 it can be seen that the angular spatial frequency measured at the observer β (cpr) is related to α by

$$\beta = \frac{|L - L_i|}{|L_i|} \alpha \qquad (8)$$

where L and L_i are the distances between the surface S and the observer and z_i and the image, respectively. The maximal viewed frequency according (7) and (8) is given by

$$\beta_{i\_\mathrm{max}} = \frac{|L - L_i|}{|L_i|}\alpha_T. \tag{9}$$

Equation (9) determines the maximal viewing resolution due to the capture and display system and setup limitation. Another source of viewing resolution limitation is the fact that not all rays producing the image reach the viewpoint. Fig. 6 shows some rays that actually reach the viewpoint and show the sampling of a real image by the pitch p of the lenslet or pinhole array. The sampling period is p/L radians and the Nyquist frequency β_{nyq} cpr of the sampling is given by [45]

$$\beta_{\mathrm{nyq}} = \tan^{-1}\left(\frac{L}{2p}\right) \approx \frac{L}{2p}. \tag{10}$$

Finally, the maximum frequency β_{max} of the reconstructed image, viewed by the observer, is provided by either the spatial Nyquist frequency β_{nyq} or the maximum frequency β_{i_max}, whichever is the smaller

$$\beta_{\mathrm{max}} = \min(\beta_{i\_\mathrm{max}}, \beta_{\mathrm{nyq}}) = \min\left(\alpha_T\frac{|z_i|}{|L - z_i|}, \beta_{\mathrm{nyq}}\right). \tag{11}$$

C. Depth of Field

Since with an II system only a single plane is used to capture and display the 3-D image, it is not possible for all objects to be in focus. Therefore, blurred images of objects or parts of the object that are out of the focus are obtained. The longitudinal (axial) range in which sharp images of 3-D objects can be obtained is characterized by the depth-of-field (DOF) of the system, which is usually defined as the extent of axial interval in which the PSF is higher than $1/\sqrt{2}$ times its maximum value. Let us first assume that the finite lenslets DOF is the bottleneck of the DOF of the overall II system. In such a case it can be shown [41] that the DOF of the II system is given by

$$D = 4\lambda\left(\frac{L_i}{w_l}\right)^2 \tag{12}$$

where λ is the wavelength and L_i is the distance between the lenslet array and lenslet image plane, which is assumed to be much larger than the lenslet array size w_l. If we assume that the resolution is limited by lenslets' diffraction, then the maximum resolution R, in lines/mm, is given by $R = w_l/2\lambda L_i$ [41]. Hence, it can be seen that regardless of

lenslet size and focal length, the product of depth of focus and the resolution squared (PDRS) is a constant given by

$$DR^2 = \frac{1}{\lambda}. \tag{13}$$

Equation (13) indicates that there is a tradeoff between the DOF and the resolution; therefore, the PDRS [41], [42], [58] was used as a figure of merit of an II system.

Equation (13) holds in the diffraction limited case. Often the resolution is limited by the sensor pixel size p_{pxl}. In such a case, $R = g/(L_i p_{\mathrm{pxl}})$, which, if combined with (1) and (12) yields in the paralaxial range [5]

$$DR^2\theta_d^2 = \frac{\lambda}{p_{\mathrm{pxl}}^2}. \tag{14}$$

In Section III-A, we have explained that the lenslet exit angle θ_d determines the viewing geometry specifications (VZ, GVZ, VA_i, VF_o, and VA_o) of a conventional II system. Equation (9) implies again that there is tradeoff between the resolution, DOF, and the viewing/visual range. One cannot increase one of these parameters without decreasing at least one of the other two. Note that in the pixel limited case, the tradeoff defined by (14) is irrespective to the lenslet parameters.

Equations (13) and (14) were obtained under the assumption that the lenslet is the primary DOF limiting source. For the general case, (13) and (14) serve as upper bounds and the following "uncertainty" relations can be written:

$$PDRS \le \frac{1}{\lambda} \tag{15}$$

and

$$DR^2\theta_d^2 \le \frac{\lambda}{p_{\mathrm{pxl}}^2}. \tag{16}$$

D. Information Capacity

The tradeoffs set by (13)–(16) show that one cannot independently improve one of the system parameters (DOF, resolution, object or image viewing angles, viewing zone, and visual zone) without affecting others. These tradeoffs are due to the finite information capacity of an II system. In [55], the use of the Shannon number of the system as a global figure of merit has been proposed. The Shannon number is referred to as the number of numbers required to completely determine a signal. For a system, it equals the number of spatial degrees of freedom or the number of modes. For a given signal-to-noise ratio (SNR), the Shannon number is proportional to the total information of the system. With respect to a 3-D imaging system, such as II systems, the Shannon number
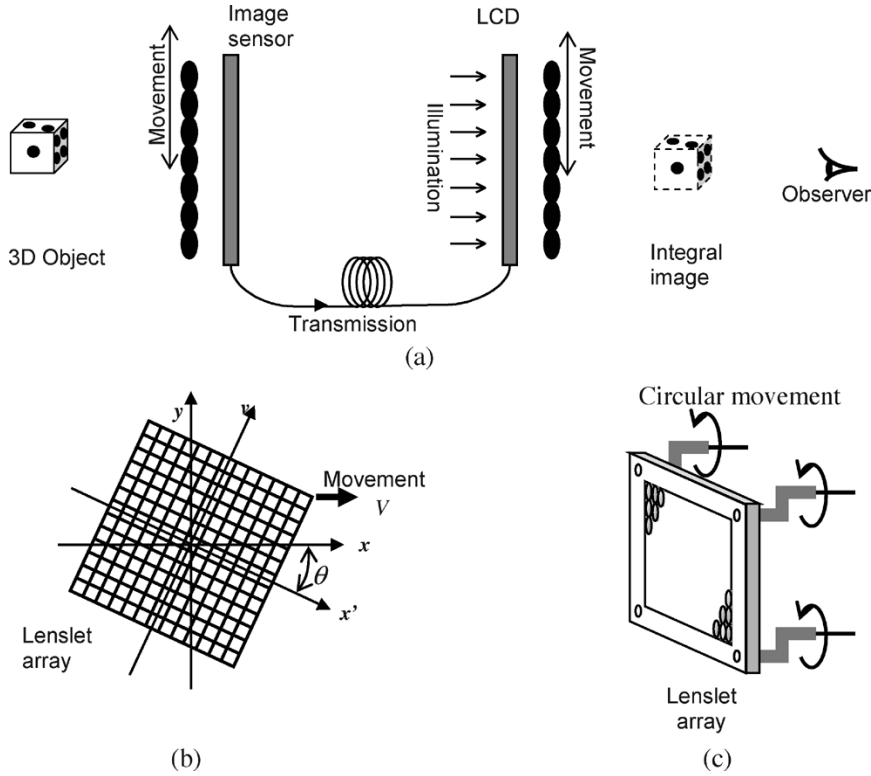
Fig. 7. (a) II with MALT. (b) Movement of tilted lenslet array to improve resolution in both x and y directions. (c) Circular movement.

of the systems defines the maximum number of voxels (volumetric pixels) that can be imaged. The Shannon number S_c of the II capturing subsystem using a lenslet array is given by [55]

$$S_c = 4N_c \tan^{-1}\left(\frac{w_c}{2g_c}\right)\alpha_c \qquad (17)$$

where α_c is given by (2) and N_c is the number of elemental images per dimension . Equation (17) is obtained from the analysis of the capture process in one dimension; for 2-D II systems, the Shannon number for both dimensions needs to be multiplied. A similar expression to (17) exists for the II display subsystem but with the respective parameters N_d, w_d, g_d, and α_d. Often, as in the case of Fig. 5(b), the pixel size is the primary resolution limitation source [59]; i.e., $\alpha_{cd} < \alpha_{cdiff} < \alpha_{cerrf}$ so that $\alpha_c = \alpha_{cd}$. In such a case, it can be shown [55] that $S_c \approx N_c$, meaning that the Shannon number is approximately the number of sensor pixels.

With an II system that has identical display and pickup subsystems, the Shannon number of the overall system is given by (17). If the pickup and display subsystem are not identical, then the Shannon number of the overall system is dictated by the subsystem that has the lower Shannon number. The expression for the Shannon number in such a case can be found in [55].

IV. MULTIPLEXING METHODS FOR INCREASING THE CAPTURED AND DISPLAYED INFORMATION

We have seen in Section III-C that there is a tradeoff between the performance parameters of an II system. This tradeoff is due to the finite information (Shannon number) that can be captured and displayed by the system with one shot. Therefore, in order to improve the II system performance, the Shannon number of the system needs to be increased. This can be done by multiplexing—that is, by taking multiple images of the same object.

A. Time-Division Multiplexing (TDM)

Several TDM schemes were proposed [13], [14], [18], [20], [21], [56], [60]–[62] to alleviate the paradigm set by the tradeoff between resolution, depth-of-field and viewing and visual parameters. With time multiplexing, motion during capture and projection is exploited to: 1) capture and display a denser optical data field representing the 3-D; that is, denser light rays from more directions captured and continued from surface S in Fig. 1, or 2) to generate an enlarged synthetic array aperture, that is, synthetically enlarging the surface S in Fig. 1(b).

In [13], a moving lenslet array technique (MALT) is proposed in which the positions of the lenslet arrays for both pickup and display are rapidly vibrated synchronously in the lateral directions within the retention time of the afterimage (or faster than the flicker fusion frequency) of the human eye. Fig. 7(a) depicts an II system using MALT. As the lenslet array moves, the elemental images change and have different perspectives within one lenslets pitch. Hence, the array pitch p is virtually decreased, yielding a higher lateral resolution according to (10) and (11). The vibration (or movement) range need not be larger than one lenslet pitch in both lattice directions, because the lenslet arrays are periodic. The elemental image detection device (CCD array) and
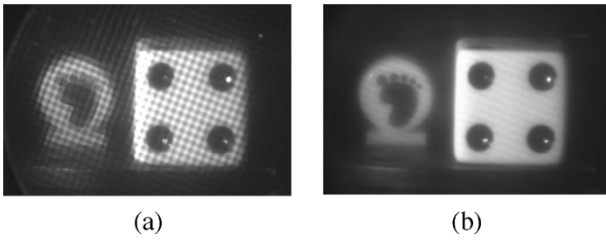
Fig. 8. Example of resolution improved by MALT. Images obtained (a) without and (b) with MALT.

the image display device (LCD or SLM) are stationary. Because the pickup lenslet array and the display lenslet array vibrate synchronously and human eyes have the effect of an averaging detector, observers therefore see a stationary reconstructed image with improved viewing resolution for a stationary object.

In general, 2-D motions are necessary to increase the spatial sampling rate along mutually orthogonal two directions in the lenslet array plane. However, for the lenslet array packed in a square, the sampling rate along the two lattice directions can be increased using linear motion by tilting the lenslet array so that the there are motion components in both lattice directions. This case is depicted in Fig. 7(b). The motion velocity needs to be adjusted so that a gap of pitch size could be scanned during the eye integration period [42]. For practical applications, a circular motion of the lenslets could be used as depicted in Fig. 7(c). In this case, the radius of the circular motion should be larger than one half pitch of the lenslets.

The resolution improvement by MALT is demonstrated in Fig. 8. The die dots, which are larger than the size of each lenslet element, are distinguishable even with a stationary II process. However, the toes in the footprint figure, which are similar to or slightly smaller than the size of each lenslet element, are not clear. Using MALT, the resolution is improved and the toes can be recognized in Fig. 8(b).

The MALT concept can be implemented also with CII [18], [20], which performs a pickup process optically with MALT, and reconstructs the images computationally. A sequence of elemental image arrays are captured with a lenslet array moved in steps smaller then the lenslet array pitch thus implementing a virtual scanning process. Then the set of captured elemental images are digitally processed to synthesize high-resolution 2-D images appropriate to the desired viewing direction. With this method the synchronization between the pickup and display array is not required. Moreover, powerful digital image processing methods can be combined. Digital superresolution reconstruction methods (see for instance [63]) are ideal for processing the captured sequence of the image acquired. In [18] the inverse back projection superresolution method is applied on the sequence of elemental image arrays captured with MALT to generate improved 2-D parallel perspective images of 3-D objects. In [20] a sequence of elemental image arrays captured with MALT are digitally processed using a different approach: a computational 3-D volumetric reconstruction algorithm is developed with which images along the longitudinal axis are reconstructed with increased resolution.

The MALT technique increases the lateral resolution of the reconstructed 3-D images by virtually decreasing the array pitch. Time multiplexing of order K in each dimension, i.e., K exposures are taken with the lenslet array moved in steps of p/K, is equivalent to sampling with a lenslet array having a pitch K times smaller but without decreasing the lenslet aperture and consequently the viewing angle. Thus, β_{nyq} (10) is increased K times without scarifying the diffraction limited bandwidth α_{diff} in (3) or θ in (1). Alternatively, a tradeoff can be made between the resolution enhancement and the viewing angle. If an array with large pitch is used then the viewing angle can be increased, since the lenslet $F\#$ is decreased. However, in such a case the resolution is scarified because the spatial sampling rate of the ray information is reduced. The loss of the resolution can be compensated by MALT [62], thus obtaining images with enlarged viewing angle without loss of lateral resolution.

A tradeoff can also be made between the resolution gained by MALT and the depth of focus [42], [64] by using nonuniform lenses to be described in Section V-C.

MALT was shown to be useful for improving the accuracy of computational evaluation of depth of object [21]. Since the depth information resolution is linearly proportional to the lateral resolution of the captured field [21], an increase of the lateral resolution of the captured elemental images obtained using MALT yields a respective increase of depth resolution. In [21] high-resolution elemental images are obtained by applying a digital numerical superresolution technique on a set of elemental images captured with MALT which yield improved depth evaluation. Consequently, improved sensing, detecting, and recognition of 3-D objects by CII is demonstrated in [21].

Another time-multiplexing technique is the synthetic aperture II (SAII) [14]. With SAII the detector and display are moved together with the lenslet arrays synchronously. The motion speed is typically set to cover at least one pitch within one exposure of the CCD. By this, the effective aperture of the lenslet is increased synthetically. As a result the object visual field is increased and the resolution of diffraction limited images is improved. In [56] the SAII concept is used together with computational reconstruction of the integral images. An enlarged effective lenslet array is obtained by capturing multiple IIs with relatively large displacement in a plane perpendicular to the optical axis. The multiple elemental images obtained are combined together to create a synthetic aperture integral image that has an enlarged effective VF_o and VA_o.

With TDM techniques the increase of the spatial sampling rate of ray information by lenslets is achieved in time; therefore, for video applications the TDM rate (the rate at which the images are taken and displayed) needs to be adjusted. If video streams with dynamic properties (ability to image moving objects) equivalent to conventional TV and video systems are desired, the capturing and displaying 25 or 30 frames per second (depending on the system), then for TDM II the rate needs to be increased properly [42]. This of course requires fast capturing and display devices. If the frame rate is increased by a factor K to achieve K-order
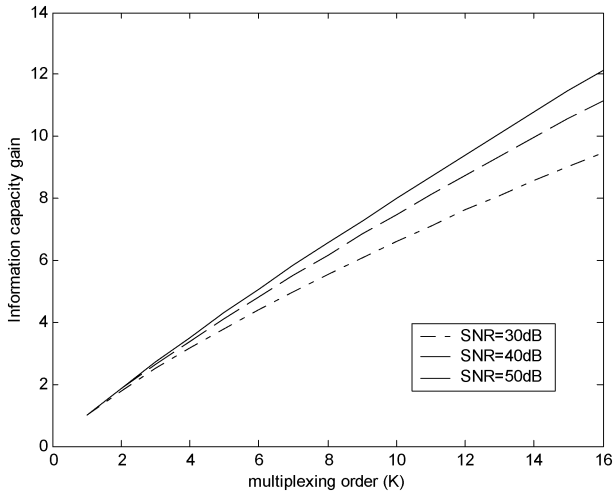
Fig. 9. Information capacity gained by K-order multiplexing for the case that the total exposure time cannot be increased, plotted for different camera SNRs.

multiplexing, the total information captured and displayed can be increased up to K times. However, even with proper setup design and using of high-quality fast imaging devices, the information capacity gained by TDM is practically less than K due to the fact that high frame rate involves low exposure time, which reduces the SNR. With typical imaging conditions it can be shown [65] that the information capacity gained by TDM is $K(1 - (\log_2 \sqrt{K} / \log_2 \mathrm{SNR}_0))$ where SNR_0 denotes the SNR of a single exposure at regular frame rate. Fig. 9 shows a graph of the information capacity gained by K-order TDM with systems that need to increase the frame rate K times. It can be seen that the multiplexing efficiency (information capacity gain divided by K) decreases with the multiplexing order K and is inversely proportional to the camera's SNR. For instance for $K = 16$ the multiplexing efficiency is 75% for a low noise camera ($\mathrm{SNR} = 50$ dB) and is lower for noisier cameras. Clearly, for still imaging of stationary objects, the frame rate constraint is not relevant and the exposure time does not need to be reduced, thus the information capacity gain can be as high as K.

B. Space-Division Multiplexing

Spatial multiplexing can be adopted to increase the 3-D image depth, viewing and visual angles, or image size. Multiple II systems with different VF_o and VZ can be combined to operate as an equivalent 3-D imaging system with enlarged viewing and visual zone. For example, if two objects are positioned out of the focus of the lens array, a clear 3-D image cannot be realized with a single II system. However, if the rays emerging from each object are directed using a beam splitter to two II systems, each focusing at one of the objects, then both objects can be captured and displayed together [66]. Although such a system requires setup alignment, it provides additional flexibility. Spatial multiplexing by using multiple display devices can also be combined with masking techniques (to be described in Section V-A) to increase the viewing angle [67].
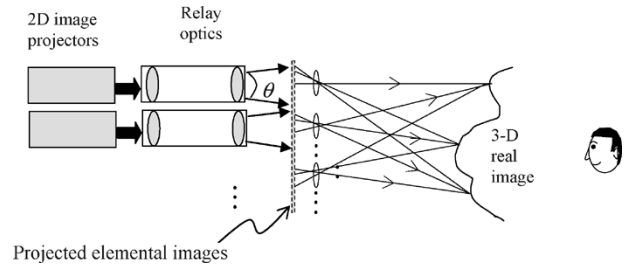

Fig. 10. Projection type II reconstruction.

C. Spatiotemporally Multiplexed II Projector

In Section III it was mentioned that typically it is the number of recording pixels that limits the amount of information captured with an II system. The same source of limitation, and even a more serious one, exists with the display device; the display resolution and size limits the total number of voxels displayed. In order to produce high-quality 3-D images with large VZ, large VA_i, large DOF, and high resolution, elemental images with a large number of pixels are required. A possible solution of the pixel number problem is by using a projection type of II [68] with spatial multiplexing [34], [69], [70]. In spatial multiplexing, many display panels (or 2-D projectors) are used for the entire elemental image display as depicted in Fig. 10. Each projector casts only a subset of the entire elemental image array onto the corresponding lenslet array part. Of course the projection angle θ should be close to zero. To alleviate the need for a large number of display panels or 2-D projectors, a temporal multiplexing scheme can be adopted [69] with which a scanning mirror is used to direct the image projected from one projector into the corresponding area of the screen (or the lenslet array) sequentially in the time domain. The high-resolution elemental images that can be displayed with such a scheme improve the resolution of the reconstructed 3-D image and density of the viewing zones. In addition, it allows the use of micromirror arrays instead of lenslet arrays, which, as explained in next section, can reproduce larger viewing zones.

V. II Systems With Nonconventional Devices For Improving Performance

A. Special Devices for Avoiding Interference

As mentioned in Section III-A, interference, or elemental image overlapping, occurs when rays from adjacent lenslets converge at the same point, within the same elemental image. In such a case different points in the object space are recorded in the same elemental image point and cannot be separated properly during the 3-D image reconstruction. As a result, double-reconstructed images are obtained. Thus, it is essential to limit the elemental image within the capture and display plane to its assigned lenslet in the pickup and display lenslet array. One method to avoid interference is by using a graded index lens array instead of the conventional lenslet array [12]. Graded index lens arrays have an additional advantage because they produce orthoscopic images and therefore pseudoscopic–orthoscopic conversion is not required.

However, they are inferior to lenslets in their imaging quality. A more common method to avoid interference is by using optical barriers [12], [37], [71] that masks elemental images from rays collected by adjacent lenslets. For increasing the VF_o and VZ a dynamic barrier together with a time division multiplexing scheme can be used. In [71] a dynamic barrier array that distributes the 3-D images to different directions in a time-division-multiplexed manner is demonstrated for increasing the number of viewing zones. By tilting the barrier array with enough speed to induce afterimage effect and synchronizing the display of the assigned elemental images, the effective VZ is increased; observers located in a wider range can view the 3-D images simultaneously.

B. Special Elements for Improving Viewing and Visual Performance (Reducing $F\#$ Limitation)

In Section III-A it was shown that the lenslet $F\#$ plays a central role in defining the viewing and visual properties (VZ, GVZ, VA_i, VF_o, VA_o,) of a conventional II system. To enlarge the viewing angle, viewing zone and visual field, the $F\#$ should be as low as possible. However, high-quality lenslets with low $F\#$ are difficult to manufacture. Typical viewing angles (VA_i and VA_o) obtained with high-quality lenses are about $10°$–$20°$. Even with an $F\#$ as low as 1, θ_d in (1) is limited by approximately $50°$. Satisfactory field of view for typical displays should be at least $60°$ [72]. Several variations of the conventional II system were proposed to enhance the viewing and visual parameters. As already mentioned in Section IV, multiplexing methods such as MALT and double device were found useful for increasing the VA_o, VA_i, VZ, and VF. Those methods were found effective, but they increase the complexity of the system; they require mechanical movement or multiplicity of devices involving careful alignment. Alternative methods for increasing the viewing and visual parameters are by using special elements in the II system as described bellow.

1) Fresnel Lens Array: One attempt to widen the viewing angle is by using a Fresnel lens array [73]. Fresnel lenses can be made with a smaller $F\#$ than lenslet arrays. However, the Fresnel lenses induce typical image distortion and there is a limitation in decreasing the f-number.

2) Lens Switching: Another method to increase θ_d is using lens switching to double the region of each elemental image [74], [75]. This approach, however, needs a mechanical mask that should move fast enough to obtain after-image effect, which causes some problems such as air resistance and noise. These problems can be avoided by using dynamic masks that use a orthogonal polarization switching method [76], [77] rather than mechanical movement. This method uses orthogonally polarized elemental images with a polarization shutter screen and the orthogonal polarization sheet attached to the lens array. The disadvantage of this method is that the intensity of the original image is reduced by half when using the polarization sheet, and consequently the integrated image becomes dim.

3) Volume Holographic Recording: Another method, which uses volume holographic recording of the elemental images [30], [78], has been proposed. A phase-conjugate beam is employed to read out elemental images stored in photorefractive volume holographic storage. However, the method cannot implement dynamic color display and the system is much more complex.

4) Microconvex-Mirror Arrays: Apparently the most efficient method is by use of micromirror arrays instead of lenslet arrays [34], [79]. Microconvex mirrors with a small f-number and negligible aberration are much more easily manufactured than similar lenslets. Each mirror element can have an $F\#$ smaller than 1. For example, if $F\# = 0.5$, the viewing angle becomes $90°$, which is acceptable for many large-scale applications. In [34] several schemes for pickup and display systems using microconvex-mirror arrays were proposed. A projection type II display system (Fig. 10) that uses microconvex mirrors with a viewing angle larger than $60°$ was demonstrated.

Additional advantages of II using microconvex mirrors are as follows.

1) They do not rotate the elemental image around its optical axis in the 3-D image reconstruction; therefore, the image obtained is orthoscopic and pseudoscopic–orthoscopic conversion is not required.
2) Flip-free observations of 3-D images are possible even if optical barriers are not used because each elemental image can be projected onto only its corresponding microconcave mirror.
3) It is easy to realize 3-D movies with large screens even if a small size of display panels or film is used. This is because the display panel and the screen are separated, and thus the size of elemental images that are projected onto the screen can be controlled easily by use of relay optics.
4) It is easy to implement spatial multiplexing or spatiotemporal multiplexing methods described in Section IV-C for displaying a large number of pixels.

In principle there is no need to use microconvex-mirror arrays both for pickup and display; II systems that combine planar lenslet arrays for pickup with a microconvex-mirror array for display, or *vice versa*, can be realized. However, it should be noted that in such cases a proportion distortion of the image occurs because a longitudinal magnification (or demagnification) takes place, whereas the lateral size does not change. This problem can be solved by using digital zoom [14], [21] or nonplanar micromirror arrays [14] described in the next subsection.

C. Special Lens Arrays

Conventional II systems use a lenslet array or an aperture array. Lenslet arrays are preferred over aperture plate arrays as they can be made to have a larger viewing area at the same resolution and have lower loss [45]. In the previous subsection, we have seen that lenslet arrays other than micromirrors and Fresnel lenslets may be beneficial. Several other than conventional lens arrays were suggested for different purposes.

1) Curved Arrays: If the planar lenslet array in the conventional II system is replaced with a curved lenslet or curved micromirror array several benefits may be gained [15], [43].
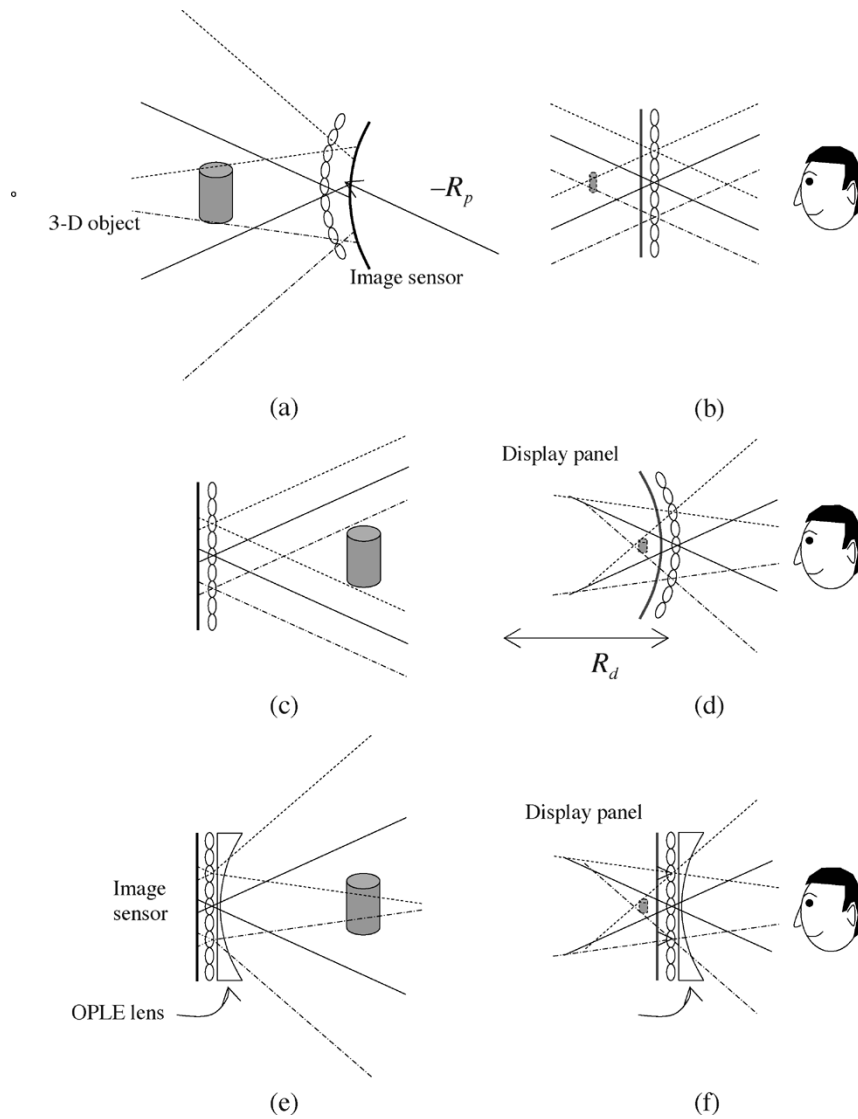
Fig. 11. II using curved devices. (a) Pickup of elemental images using curved devices. (b) 3-D image reconstruction using planar devices. (c) Pickup of elemental images using planar devices. (d) 3-D image reconstruction using curved devices. (e) Equivalent setup to curved pickup devices. (f) Equivalent setup to curved display devices.

In [43] it is shown that a curved lenslet array in the display system used with elemental images generated by CGII can remarkably improve the VA_i. This is because with a curved lenslet array every viewing point outside the viewing zone can be made available for sharp azimuthal viewing angles by integrating images from eccentric elemental images (close to the edges) that are normally masked by the optical barrier with the conventional II. However, in the implementation in [43], a "gap mismatch" problem occurs due to varying gap between the curved lens array and the flat display panel, which induces distortions in the reconstructed image.

In [15], a method is presented which uses a curved pickup lenslet array or a curved microconvex-mirror array (Fig. 11), or both, for controlling the depth and size of the reconstructed 3-D images in II. With lateral and longitudinal magnification control, it is possible to pick up large 3-D objects that may be far away and then to display their 3-D images of a reduced size within the depth-of-focus of the II systems. This feature is especially important for practical 3-D displays including

3-D television, video, and movie, where typically large 3-D objects that may be far away, such as nature scenes, need to be displayed to a viewer located close to the display system.

The operation principle of the method can be understood through Fig. 11(a) and (b). By using a negatively curved pickup lenslet array, the disparity of neighboring elemental images increases because pickup directions of the lenslets in a curved array are not parallel and thus their fields of view are more separated than those for a planar array. Such elemental images are equivalently obtained if we pick up the object of a reduced size near the pickup lenslet array. Therefore, when elemental images with increased disparity are displayed on a planar display screen (a microconvex-mirror array), an integral image with a reduced size is reconstructed near the screen [Fig. 11(b)]. Thus, image size can be controlled by varying the curvature of the lenslet array R. In this method, as the object distance increases, the longitudinal image depth reduces in a nonlinear way, while the lateral size reduces in a linear way. To reduce the depth of reconstructed images

alone, a method to zoom elemental images in can be used. In the experiment reported in [15], a planar pickup device together with an additional large aperture negative lens in contact with the pickup lenslet array is used, which are shown to be functionally equivalent to the curved pickup devices [Fig. 11(e) and (f)].

2) Nonuniform Lens Array: A possible way to increase the 3-D image DOF is to use an array with varying focal lengths and aperture sizes [42], [80]. Lenses with different focal lengths contribute to different image depth cross sections. When a suitable nonuniform lenslet array is used it is possible to improve the DOF of 3-D images. The nonuniform lenslet array consisting of groups of lenslets of varying focal length and lenslet size packed in a periodic pattern, which can be viewed as a superposition of uniform lenslet arrays, each designed to focus on a different depth range and resolution. However, the subarrays have a lower pitch and possibly low aperture; therefore, according to (3) and (10), each depth cross section can be imaged with low lateral resolution. MALT can be used here also to remedy the loss of lateral resolution [42]. Another disadvantage of this method is that care needs to be taken to block the area between the lenses, which causes light loss.

3) Amplitude Modulated Lenslet Array: In [58], a technique is presented for improving the depth of field without reducing the spatial resolution. The technique is based on modulating the amplitude transmittance of the lenslets. It is shown that by simply obscuring the central part of the lenslets, the PDRS of an integral-image system can be increased almost by 400%. However, the price that is paid with this technique is reduction of the light efficiency and distortions due to increased aberrations of the partially blocked lenslets.

4) Electronically Synthesized Lenslet Array (ESLA): Mechanical movement in the MALT method (see Section IV-A) can be avoided by replacing the lenslet array with an ESLA [81]. For an ESLA, an array of Fresnel zone plates is generated in an LCD. Each lenslet is obtained by turning the LCD pixels on and off according to the zone-plate pattern calculated with a PC. In such a way the position of the lenslet array realized by ESLA can be controlled electronically in real time without need of mechanical movement. However, the method suffers from poor contrast and poor light efficiency due to performance limitations of spatial light modulators available today.

5) Arrays With Nonrectangular Grids: Most common lenslet or aperture plate arrays are arranged in a rectangular (square) grid. But there is no restriction for the arrays to have a rectangular grid. On the contrary, it has been shown that nonrectangular grids are useful for reducing the moiré effects in contact type 3-D imaging displays [82], [83]. Such systems use a flat panel display layered with a grid-type optical plate such as a microlens array or parallax barrier plate. Moiré patterns may appear due to the superposition of the two grid-type devices. It was found that the moiré effect can be minimized if the rectangular lenslet array is replaced by a cross-lenticular plate, which is composed of two lenticular plates, crossed at angles between $20°$ and $30°$.

VI. CONCLUSION

II is a promising 3-D imaging technique as it can provide multiview autostereoscopic 3-D images with a relatively simple and compact system that does not require special viewing devices and imaging requirements. These features make II an excellent candidate for implementation in professional and commercial applications that could benefit from 3-D imaging. Some practical implementations were proposed already, but in order to be widely used in daily life the resolution-DOF-viewing angle paradigm must be overcome. This paradigm can be shortly expressed through the "uncertainty principles" given in Section III-C. It is a result of using 2-D recording, displaying devices, and optical devices to represent enormous amount of information representing 3-D optical data.

Nevertheless, with upcoming technology together with multiplexing techniques and methods described in this paper, the paradigm can be expected to be broken and II systems will reach a level required for wide-scale application. Let us consider, for instance, the example of Fig. 5(a): with the availability of a pickup sensor pixel size of 1.4 μm, the sensor resolution limitation can be relaxed to the order of the optical resolution limitation; $\alpha_{cd} \approx \alpha_{cdiff} = 1800$ cpr. If, in addition, a 20-megapixel sensor together with multiplexing of order 4 can be efficiently implemented, a 80-megavoxels 3-D image could be captured. This amount of information could represent, for instance, an equivalent of about 260 completely independent VGA-resolution views, which actually are equivalent to a much larger number of correlated views, since the views of 3-D objects are highly redundant. The large amount of information involved in 3-D imaging need to be manipulated efficiently in order to produce 3-D images with desired specifications, that is, to control the resolution, DOF, and viewing and visual geometrical parameters. For this purpose, techniques as described in Section V can be useful. Another challenge that rises with the huge amount of information is the necessity to efficiently store and transmit the data. For this, efficient compression techniques need to be developed. Several techniques of II compression were proposed already [23], [24], [84] demonstrating good quality compression with a compression ratio of up to 130.

In conclusion, with future generations of 2-D sensing and display systems to come, combined with techniques similar to those presented in this paper it is not unlikely that II will reach a level of implementation in various consumer and professional applications. Remaining challenges are further improvement of capture and display technology and developing methods to process and store the huge amount of data required to image 3-D scenes. Efforts to efficiently control 3-D image resolution, depth-of-focus, and viewing and visual geometry should be pursued also.

This paper is dedicated to the memory of Dr. Ju-Seog Jang (1961–2004).

REFERENCES

[1] L. Lypton, *Foundation of Stereoscopic Cinema, A Study in Depth.* New York: Van Nostrand Reinhold, 1982.

[2] T. Okoshi, "Three-dimensional displays," *Proc. IEEE,* vol. 68, no. 5, pp. 548–564, May 1980.

[3] T. Yamazaki, K. Kamijo, and S. Fukuzumi, "Quantitative evaluation of visual fatigue encountered in viewing stereoscopic 3-D display—near point distance and visual evoked potential study," in *Proc. Japan Display '89,* pp. 606–609.

[4] A. Stern and B. Javidi, "Ray phase space approach for 3-D imaging and 3-D optical data representation," *IEEE/OSA J. Display Technol.,* to be published.

[5] ——, "3-D imaging with lenslet arrays," *Proc. SPIE, Optical Information Systems III,* vol. 5908, pp. 118–131, 2005.

[6] M. G. Lippmann, "Epreuves reversibles donnant la sensation du relief," *J. Phys.,* vol. 7, pp. 821–825, Nov. 1908.

[7] H. Arimoto and B. Javidi, "Integral three-dimensional imaging with digital reconstruction," *Opt. Lett.,* vol. 26, pp. 157–159, Feb. 2001.

[8] T. Okoshi, *Three-Dimensional Imaging Techniques.* New York: Academic, 1976.

[9] A. P. Sokolov, *Autostereoscpy and Integral Photography by Professor Lippmann's Method.* Moscow, Russia: Moscow State Univ. Press, 1911.

[10] H. E. Ives, "Optical properties of a Lippmann lenticuled sheet," *J. Opt. Soc. Amer.,* vol. 21, pp. 171–176, Mar. 1931.

[11] F. Okano, H. Hoshino, J. Arai, and I. Yuyama, "Real-time pickup method for a there-dimensional image based on integral photography," *Appl. Opt.,* vol. 36, pp. 1598–1603, Jul. 1997.

[12] J. Arai, F. Okano, H. Hoshino, and I. Yuyama, "Gradient-index lenss-array method based on real time integral photography for three-dimensional images," *Appl. Opt.,* vol. 7, pp. 2034–2045, Jul. 1998.

[13] J. S. Jang and B. Javidi, "Improved viewing resolution of 3-D integral imaging with nonstationary micro-optics," *Opt. Lett.,* vol. 27, pp. 324–326, Mar. 2002.

[14] ——, "Three-dimensional synthetic aperture integral imaging," *Opt. Lett.,* vol. 27, pp. 1144–1146, Jul. 2002.

[15] ——, "Depth and lateral size control of three-dimensional images in projection integral imaging," *Opt. Express,* vol. 12, pp. 3778–3790, Jul. 2004.

[16] Y. Frauel and B. Javidi, "Digital three-dimensional image correlation using computer-reconstructed integral imaging," *Appl. Opt.,* vol. 41, pp. 5488–5496, Sep. 2002.

[17] T. Naemura, T. Yoshida, and H. Harashima, "3-D computer graphics based on integral photography," *Opt. Express,* vol. 8, pp. 255–262, Feb. 2001.

[18] A. Stern and B. Javidi, "Three-dimensional image sensing and reconstruction with time-division multiplexed computational integral imaging," *Appl. Opt.,* vol. 42, pp. 7036–7042, Dec. 2003.

[19] J. S. Jang and B. Javidi, "Three-dimensional volumetric object reconstruction using computational integral imaging," *Opt. Express,* vol. 12, pp. 483–491, Feb. 2004.

[20] S. H. Hong and B. Javidi, "Improved resolution 3-D object reconstruction using computational integral imaging with time multiplexing," *Opt. Express,* vol. 12, pp. 4579–4588, Sep. 2004.

[21] S. Kishk and B. Javidi, "Improved resolution 3-D object sensing and recognition using time multiplexed computational integral imaging," *Opt. Express,* vol. 11, pp. 3528–3541, Dec. 2003.

[22] J. H. Park, Y. Kim, J. Kim, S. W. Min, and B. Lee, "Three-dimensional display scheme based on integral imaging with three-dimensional information processing," *Opt. Express,* vol. 12, pp. 2032–6020, Nov. 2004.

[23] R. Zaharia, A. Aggoun, and M. McCormick, "Adaptive 3D-DCT compression algorithm for continuous parallax 3-D integral imaging," *Signal Process. Image Commun.,* vol. 17, pp. 231–242, Sep. 2002.

[24] S. Yeom, A. Stern, and B. Javidi, "Compression of color integral images using MPEG 2," *Opt. Express,* vol. 12, pp. 1632–1642, Mar.. 2004.

[25] Y. Frauel, E. Tajahuerce, O. Matoba, A. Castro, and B. Javidi, "Comparison of passive ranging integral imaging and active imaging digital holography for three-dimensional object recognition," *Appl. Opt.,* vol. 43, p. 452, 2004.

[26] S. Yeom and B. Javidi, "Three-dimensional distortion-tolerant object recognition using integral imaging," *Opt. Express,* vol. 12, pp. 5795–5809, Nov. 2004.

[27] Y. Heiser, A. Stern, and B. Javidi, Recognition of Three-Dimensional Objects Having Arbitrary Orientation Using Integral Imaging in preparation.

[28] O. Matoba, E. Tajahuerce, and B. Javidi, "Real-time three-dimensional object recognition with multiple perspectives imaging," *Appl. Opt.,* vol. 40, pp. 3318–3326, Jul. 2001.

[29] ——, "Tree-dimensional display and recognitions system based on multiple perspectives integral imaging," in *Three-Dimensional Television, Video, and Display Technology* B. Javidi and F. Okano, Eds. Berlin Heidelberg, NY: Springer-Verlag, 2002, pp. 241–256.

[30] S. H. Shin and B. Javidi, "Real time three dimensional integral imaging display and object recognition using volume optical storage," in *Three-Dimensional Television, Video, and Display Technology,* B. Javidi and F. Okano, Eds. Berlin Heidelberg, NY: Springer-Verlag, 2002, pp. 143–166.

[31] J.-S. Jang and B. Javidi, "Three-dimensional integral imaging of micro-objects," *Opt. Lett.,* vol. 29, pp. 1230–1232, 2004.

[32] T. Wilson, Ed., *Confocal Microscopy.* London, U.K.: Academic, 1990.

[33] L. Hongen, N. Hata, S. Nakajima, M. Iwahara, I. Sakuma, and T. Dohi, "Surgical navigation by autostereoscopic image overlay of integral videography," *IEEE Trans. Inf. Technol. Biomed.,* vol. 8, pp. 114–121, Jun. 2004.

[34] J.-S. Jang and B. Javidi, "Three-dimensional projection integral imaging using micro-convex-mirror arrays," *Opt. Express,* vol. 12, pp. 1077–1086, Mar. 2004.

[35] ——, "Two-step integral imaging for orthoscopic three-dimensional imaging with improved viewing resolution," *Opt. Eng,* vol. 41, pp. 2568–2571, Oct. 2002.

[36] N. Davies, M. McCormick, and L. Yang, "Three-dimensional imaging systems: a new development," *Appl. Opt.,* vol. 27, pp. 4520–4528, 1988.

[37] J.-H. Park, S.-W. Min, S. Jung, and B. Lee, "Analysis of viewing parameters for two display methods based on integral photography," *Appl. Opt.,* vol. 40, pp. 5217–5232, Oct. 2001.

[38] J.-S. Jang and B. Javidi, "Formation of orthoscopic three-dimensional real images in direct pickup one-step integral imaging," *Opt. Eng.,* vol. 42, pp. 1869–1870, Mar. 2003.

[39] Y. Igarishi, H. Murata, and M. Ueda, "3D display system using a computer-generated integral photograph," *Jpn. J. Appl. Phys.,* vol. 17, pp. 1683–1684, 1978.

[40] S.-W. Min, S. Jung, J.-H. Park, and B. Lee, "Three-dimensional display system based on computer generated integral photography," in *Proc. SPIE, Stereoscopic Displays and Virtual Reality Systems VIII* A. J. Woods, J. O. Merritt, and S. A. Benton, Eds., 2001, vol. 4297, pp. 187–195.

[41] J.-S. Jang, F. Jin, and B. Javidi, "Three-dimensional integral imaging with large depth of focus by use of real and virtual image fields," *Opt. Lett.,* vol. 28, pp. 1421–1423, Aug. 2003.

[42] J.-S. Jang and B. Javidi, "Time-multiplexed integral imaging: for 3-D sensing and display," *Opt. Photon. News,* vol. 15, pp. 36–43, Apr. 2004.

[43] Y. Kim, J.-H. Park, H. Choi, S. Jung, S.-W. Min, and B. Lee, "Viewing-angle-enhanced integral imaging system using a curved lens array," *Opt. Express,* vol. 12, pp. 421–329, Feb. 2004.

[44] C. B. Burckhardt, "Optimum parameters and resolution limitation of integral photography," *J. Opt. Soc. Amer.,* vol. 58, pp. 71–76, Jan. 1968.

[45] H. Hoshino, F. Okano, H. Isono, and I. Yuyama, "Analysis of resolution limitation of integral photography," *J. Opt. Soc. Amer. A.,* vol. 15, pp. 2059–2065, Aug. 1998.

[46] J. Arai, H. Hoshino, M. Okui, and F. Okano, "Effects of focusing on the resolution characteristics of integral photography," *J. Opt. Soc. Amer. A.,* vol. 20, pp. 996–1004, Jun. 2003.

[47] J. Arai, M. Okui, M. Kobayashi, and F. Okano, "Geometrical effects of positional errors in integral photography," *J. Opt. Soc. Amer. A.,* vol. 21, pp. 951–958, Jun. 2004.

[48] M. C. Forman, N. Davies, and M. McCormick, "Continuous parallax in discrete pixelated integral three-dimensional displays," *J. Opt. Soc. Amer. A.,* vol. 20, pp. 411–421, Mar. 2003.

[49] M. Martínez-Corral, B. Javidi, R. Martínez-Cuenca, and G. Saavedra, "Multi-facet structure of observed reconstructed integral images," *J. Opt. Soc. Amer. A.,* vol. 22, pp. 597–603, Mar. 2005.

[50] ——, "Integral imaging with improved depth of field by use of amplitude modulated microlens array," *Appl. Opt.,* vol. 43, pp. 5806–5813, Nov. 2004.

[51] J.-Y. Son, V. V. Saveljev, Y.-J. Choi, J.-E. Bahn, S.-K. Kim, and H. Choi, "Parameters for designing autostereoscopic imaging systems based on lenticular, parallax barrier, and integral photography plates," *Opt. Eng.,* vol. 42, pp. 3326–3333, Nov. 2003.

[52] S.-W. Min, J. Hong, and B. Lee, "Analysis of an optical depth converter used in a three-dimensional integral imaging system," *Appl. Opt.,* vol. 43, pp. 4539–4549, Aug. 2004.

[53] J.-Y. Son, V. V. Saveljev, J.-S. Kim, S.-S. Kim, and B. Javidi, "Viewing zones in three-dimensional imaging systems based on lenticular, parallax-barrier, and microlens-array plates," *Appl. Opt.,* vol. 43, pp. 4985–4992, Sep. 2004.

[54] S. Manolache, A. Aggoun, M. McCormick, N. Davies, and S. Y. Kung, "Analytical model of a three-dimensional integral image recording system that uses circular- and hexagonal-based spherical surface microlenses," *J. Opt. Soc. Amer. A.,* vol. 18, pp. 1814–1821, Aug. 2001.

[55] A. Stern and B. Javidi, "Shannon number and information capacity of integral images," *J. Opt. Soc. Amer. A.,* vol. 21, pp. 1602–1612, Sep. 2004.

[56] ——, "3-D computational synthetic aperture integral imaging (COMPSAII)," *Opt. Express,* vol. 11, no. 19, pp. 2446–2451, Sep. 2003.

[57] F. Okano, H. Hoshino, J. Arai, M. Yamada, and I. Yuyama, "Tree-dimensional television system based on integral photography," in *Three-Dimensional Television, Video, and Display Technology*, B. Javidi and F. Okano, Eds. Berlin, Germany: Springer-Verlag, 2002, pp. 101–124.

[58] M. Martínez-Corral, B. Javidi, R. Martínez-Cuenca, and G. Saavedra, "Integral imaging with improved depth of field by use of amplitude modulated microlens array," *Appl. Opt.,* vol. 43, pp. 5806–5813, Nov. 2004.

[59] R. Martínez-Cuenca, G. Saavedra, M. Martínez-Corral, and B. Javidi, "Enhanced depth of field integral imaging with sensor resolution constraints," *Opt. Express,* vol. 12, pp. 5237–5242, Oct. 2004.

[60] L. Erdmann and K. J. Gabriel, "High resolution digital photography by use of a scanning microlens array," *Appl. Opt.,* vol. 40, pp. 5592–5599, Nov. 2001.

[61] J.-S. Jang and B. Javidi, "Improved-quality three-dimensional Integral imaging and projection using nonstationary optical components," in *Three-Dimensional Television, Video, and Display Technology*, B. Javidi and F. Okano, Eds. Berlin, Germany: Springer-Verlag, 2002, pp. 123–142.

[62] ——, "Improvement of viewing angle in integral imaging by use of moving lenslet arrays with low fill factor," *Appl. Opt.,* vol. 42, pp. 1996–2002, Apr. 2003.

[63] A. Stern, Y. Porat, A. Ben-Dor, and N. S. Kopeika, "Enhanced-resolution image restoration from a sequence of low-frequency vibrated images using convex projections," *Appl. Opt.,* vol. 40, pp. 4706–4715, Sep. 2001.

[64] J.-S. Jang and B. Javidi, "Large depth-of-focus time-multiplexed three-dimensional integral imaging using lenslets with nonuniform focal lengths and aperture sizes," *Opt. Lett.,* vol. 28, pp. 1924–1926, 2003.

[65] A. Stern and B. Javidi, "Information capacity gain by time-division multiplexing in three-dimensional integral imaging," *Opt. Lett.,* vol. 30, pp. 1135–1137, May 2005.

[66] B. Lee, S.-W. Min, and B. Javidi, "Theoretical analysis for three-dimensional integral imaging systems with double devices," *Appl. Opt.,* vol. 41, pp. 4856–4865, Aug. 2002.

[67] S. Jung, J.-H. Park, B. Lee, and B. Javidi, Viewing-Angle-Enhanced Integral 3-D Imaging Using Double Display Devices With Masks vol. 41, pp. 2389–2390, Oct. 2002.

[68] J.-S. Jang and B. Javidi, "Real-time all-optical three-dimensional integral imaging projector," *Appl. Opt.,* vol. 41, pp. 4866–4869, Aug. 2002.

[69] ——, "Spatiotemporally multiplexed integral imaging projector for large-scale high-resolution three-dimensional display," *Opt. Express,* vol. 12, pp. 557–563, Feb. 2004.

[70] H. Liao, M. Iwahara, N. Hata, and T. Dohi, "High-quality integral videography using a multiprojector," *Opt. Express,* vol. 12, pp. 1067–107 622, Mar. 2004.

[71] H. Choi, S.-W. Min, S. Jung, J.-H. Park, and B. Lee, "Multiple-viewing-zone integral imaging using a dynamic barrier array for three-dimensional displays," *Opt. Express,* vol. 11, pp. 927–932, Apr. 2003.

[72] A. R. L. Travis, "The display of three dimensional video images," *Proc. IEEE,* vol. 85, no. 11, pp. 1817–1832, Nov. 1997.

[73] S.-W. Min, S. Jung, J.-H. Park, and B. Lee, "Study for wide-viewing integral photography using an aspheric Fresnel-lens array," *Opt. Eng.,* vol. 41, pp. 2572–2576, Oct. 2002.

[74] B. Lee, S. Jung, and J.-H. Park, "Viewing-angle-enhanced integral imaging using lens switching," *Opt. Lett.,* vol. 27, pp. 818–820, May 2002.

[75] J.-H. Park, S. Jung, H. Choi, and B. Lee, "Viewing-angle-enhanced integral imaging by elemental image resizing and elemental lens switching," *Appl. Opt.,* vol. 41, pp. 6875–6883, Nov. 2002.

[76] S. Jung, J.-H. Park, H. Choi, and B. Lee, "Wide-viewing integral three-dimensional imaging by use of orthogonal polarization switching," *Appl. Opt.,* vol. 42, pp. 2513–2520, May 2003.

[77] ——, "Viewing-angle-enhanced integral three-dimensional imaging along all directions without mechanical movement," *Opt. Express,* vol. 11, pp. 1346–1356, Jun. 2003.

[78] S.-H. Shin and B. Javidi, "Viewing-angle enhancement of speckle-reduced volume holographic three-dimensional display by use of integral imaging," *Appl. Opt.,* vol. 41, pp. 5562–5567, Sep. 2002.

[79] Y. Jeong, S. Jung, J.-H. Park, and B. Lee, "Reflection-type integral imaging scheme for displaying three-dimensional images," *Opt. Lett.,* vol. 27, pp. 704–706, May 2002.

[80] J.-S. Jang and B. Javidi, "Large depth-of-focus time-multiplexed three-dimensional integral imaging using lenslets with nonuniform focal lengths and aperture sizes," *Opt. Lett.,* vol. 28, pp. 1924–1926, Oct. 2003.

[81] ——, "Three-dimensional integral imaging with electronically synthesized lenslet arrays," *Opt. Lett.,* vol. 27, pp. 1767–1769, Oct. 2002.

[82] J.-Y. Son, "3D display," *IEEE LEOS Newslett.,* vol. 18, pp. 13–14, Feb. 2004.

[83] J.-Y. Son, V. V. Saveljev, B. Javidi, and K. D. Kwack, "A method of building pixel cells with an arbitrary vertex angle," *Opt. Eng.,* vol. 44, pp. 3326–3333, Feb. 2005.

[84] E. Elharar, A. Stern, O. Hadar, and B. Javidi, A Hybrid Compression Method for Integral Images Using Discrete Wavelet Transform and Discrete Cosine Transform in preparation.

Adrian Stern received the B.Sc., M.Sc. (*cum laude*), and Ph.D. degrees in electrical and computer engineering from Ben-Gurion University of the Negev, Israel, in 1988, 1997 and 2003, respectively.

During 2002–2003, he was a Postdoctoral Fellow in the Electrical and Computer Engineering Department, University of Connecticut, Storrs. He is now with the Department of Electro-Optical Engineering at Ben-Gurion University of the Negev. His current research interests include three-dimension imaging, biomedical imaging, sequences of images processing, image restoration, superesolution, image and video compression, optical encryption, and atmospheric optics.

Bahram Javidi (Fellow, IEEE) received the B.S. degree in electrical engineering from George Washington University, Washington, D.C., and the M.S. and Ph.D. degrees in electrical engineering from the Pennsylvania State University, University Park.

He is Board of Trustees Distinguished Professor at the University of Connecticut, Storrs. He has supervised over 80 masters and doctoral graduate students, postdoctoral students, and visiting professors during his academic career. He has published over 200 technical articles in major journals. He has published over 230 conference proceedings, including over 90 invited conference papers, and 60 invited presentations. His papers have been cited over 2600 times, according to the citation index of *WEB of Science*. His papers have appeared in *Physics Today* and *Nature*, and his research has been cited in the *Frontiers in Engineering Newsletter*, published by the National Academy of Engineering, IEEE *Spectrum*, *Science*, *New Scientist*, and *National Science Foundation Newsletter*. He has completed several books including, *Optical Imaging Sensors and Systems for Homeland Security Applications* (Springer, 2005); *Optical and Digital Techniques For Information Security* (Springer, 2005); *Image Recognition: Algorithms, Systems, and Applications* (Marcel Dekker, 2002); *Three Dimensional Television, Video, and Display Technologies* (Springer-Verlag, 2002);

Smart Imaging Systems (SPIE Press, 2001); *Real-Time Optical Information Processing* (Academic Press, 1994), *Optical Pattern Recognition* (SPIE Press, 1994). He is currently the Editor in Chief of the Springer Verlag series on Advanced Science and Technologies for Security Applications. He has served as topical editor for Springer-Verlag, Marcel Dekker publishing company, *Optical Engineering Journal*, and IEEE/SPIE Press Series on Imaging Science and Engineering. He has held visiting positions during his sabbatical leave at Massachusetts Institute of Technology, United States Air Force Rome Lab at Hanscom Base, and Thomson-CSF Research Labs in Orsay, France. He is a consultant to industry in the areas of optical systems, image recognition systems, and 3-D optical imaging systems. He has active research collaborations with numerous universities and industries in the United States, Japan, South Korea, Italy, Germany, France, Ireland, United Kingdom, Egypt, Israel, Spain, and Mexico.

Dr. Javidi is a Fellow of the Optical Society of America (OSA) and Fellow of the International Society for Optical Engineering (SPIE). He was awarded the Dennis Gabor Award in Diffractive Wave Technologies by the SPIE in 2005. He was the recipient of the IEEE Lasers and Electro-Optics Society Distinguished Lecturer Award twice in 2003 and 2004. He has been awarded the University of Connecticut Board Of Trustees Distinguished Professor Award, the School Of Engineering Distinguished Professor Award, University of Connecticut Alumni Association Excellence in Research Award, the Chancellor's Research Excellence Award, and the first Electrical and Computer Engineering Department Outstanding Research Award. In 1990, the National Science Foundation named him a Presidential Young Investigator. He has served as the Chairman of the IEEE Lasers and Electro-Optics (LEOS) Technical Committee on Electro-Optics Sensors and Systems, member of the IEEE Neural Networks Council, Chairman of the Optics in Information System Working Group of Optical Engineering Society (SPIE), and Chair of the OSA Image Recognition technical Group. He has served on the program committees of more than two dozens international meetings on information systems sponsored by IEEE, OSA, SPIE, and ICO. He was awarded the IEEE Best Journal Paper Award from IEEE Transactions on Vehicular Technology in 2002. He is on the editorial board of the new IEEE Journal of Display Technologies.